ELSEVIER

Engineering Geology 41 (1996) 181–195

ENGINEERING GEOLOGY

Time-dependent behaviour of deep clays

A. Giraud *, G. Rousset

Groupement pour l'étude des Structures Souterraines de Stockage (G.3S), Ecole Polytechnique, 91128 Palaiseau Cedex, France

Received 21 February 1994; accepted 23 June 1995

Abstract

The time-dependent behaviour of deep saturated clays is related both to the effects of hydraulic diffusion and of viscosity. In this paper, we present first, by means of an experimental approach, the main features of the mechanical properties of deep clays. Then, we study the effects of these specific behaviours on the time-dependent behaviour of underground structures. We present theoretical and numerical investigations of the effects of pore pressure diffusion resulting from a tunnel excavation in a poroplastic or poroviscoplastic medium. Finite-element calculations show that the time-dependent convergence of the tunnel wall is non negligible. Then, we focus on the behaviour of a cylindrical thermal source buried in a deep clay.

Coupling effects between thermal, hydraulic and mechanical behaviours are very important in soft and low permeable deep clays (saturated compressible clays with high porosity). We show in particular that the displacements and the stresses are very sensitive to the constitutive model. Irreversible behaviour may be traduced by appearance of residual stresses within the rockmass.

1. Introduction

For many underground geotechnical problems in deep clays, time-dependent phenomena are significant. The case of the underground laboratory at Mol in Belgium (where many experimental galleries have been built 230 m deep in the plastic Boom clay), gives a very good illustration of this behaviour.

Fig. 1 shows the main results of the so called "convergence controlled lining test" in situ experiment (Rousset, 1988). The lining of this gallery

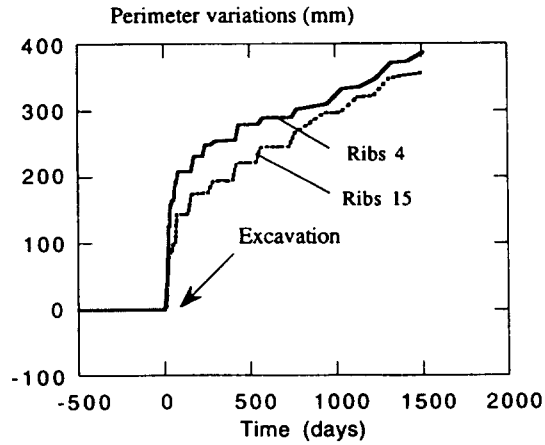

Fig. 1. In situ measurements of sliding.

* Presently at the Laboratoire de Géomécanique, ENSG, Rue du Doyen Marcel Roubault, 54501 Vandoevre-les-Nancy, France.

SSDI 0013-7952(95)00000-Q

consists of sliding ribs (Bernaud and Rousset, 1993): when the pressure P_i exerted by the surrounding rockmass on the lining exceeds a given value, convergence occurs by free sliding. Then, P_i remains approximately constant ($P_i = 1.7$ MPa for this specific dimensioning).

This figure shows that more than 60% of the convergence of the lining occurs after completion of the gallery, i.e., the major part of closure is due to time-dependent effects.

Another case of a delayed phenomenon on the same site is reported by Neerdael et al. (1991). Curve number i, plotted in Fig. 2, represents the value of the pore pressure inside the rockmass at a distance r_i from the center of a gallery ($r_{i+i} > r_i$). This gallery is lined with concrete blocks.

Before the construction of the gallery, the pore pressure field was quite stable (the hydraulic gradient observed on Fig. 2 is due to the presence of other surrounding underground works, which play the role of drains).

The pore pressure response is very sensitive to the construction: as the front progresses, pore pressure within the rockmass decreases (instantaneous response) in a manner which depends on r_i. Then, after completion of the gallery, pore pressure evolves very slowly (time-dependent behaviour). Due to hydro-mechanical couplings in porous media, this variation of the pore pressure field induces time-dependent variations of other mechanical parameters (convergence or stress for example).

These two examples illustrate very well the two

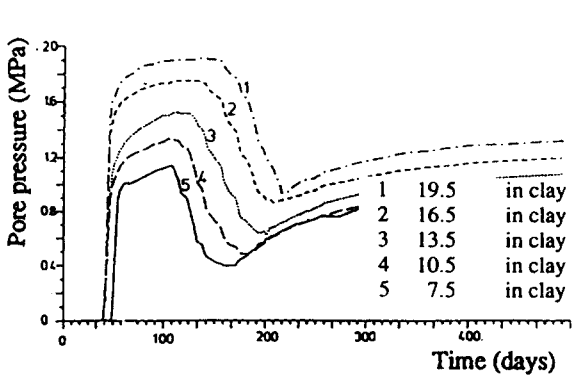

Fig. 2. Evolution of the pore pressure field around a gallery.

main causes of time-dependent effects in an underground structure: viscosity of the rockmass and hydraulic diffusion. The first cause, viscosity, is intrinsic: it depends on the constitutive model of the material and does not depend on the structure. It can be studied classically in laboratory by performing undrained creep tests. The second cause, hydraulic diffusion, is extrinsic because it depends also on the geometry and on the boundary conditions of the structure.

The purpose of this paper is to study both causes of time-dependent behaviour of deep clays and to examine their relative effects on the delayed behaviour of a structure. Moreover, attention will be paid to the influence of temperature on these behaviours.

The first part is related to experimental observations involving two different deep clays: a plastic one, that of the Boom clay formation, and a brittle one coming from the Paris basin. Then, constitutive models are proposed in the second part of the paper. Finally, by means of parametric numerical analyses, we study the effects of these specific phenomena on the time-dependent behaviour of underground structures.

2. Experimental approach

2.1. The case of Boom Clay

(a) Instantaneous behaviour: Boom clay is a very porous material (porosity $\phi \simeq 45\%$; wet density $d = 1.95$). The samples have been cored at the Mol site (Belgium), at 230 m depth. Plasticity of Boom clay is significant: undrained triaxial test results (Fig. 3) show that, under a confining stress P of 5 MPa, the deviatoric curve $(Q-P)(\varepsilon)$ reaches its maximum value of nearly 2 MPa at very high levels of axial strain, more than 5%; ductility is, therefore, a main feature of the mechanical behaviour of the material.

Moreover, the increasing part of the curve (ε small), does not correspond to a reversible process: cyclic triaxial tests performed under comparable conditions ($P = 5$ MPa) (Fig. 4) show that the major part of the deformation

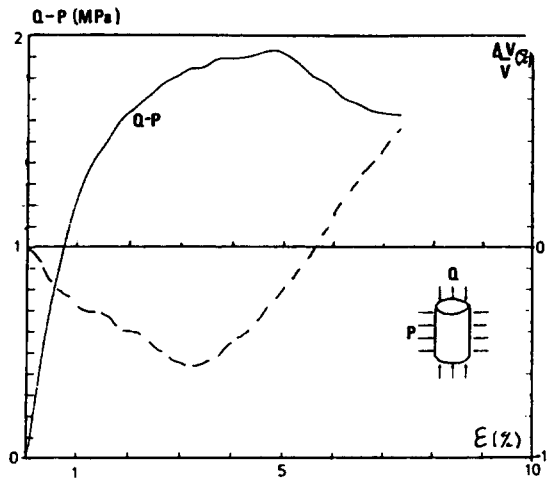

Fig. 3. Triaxial tests on Boom clay.

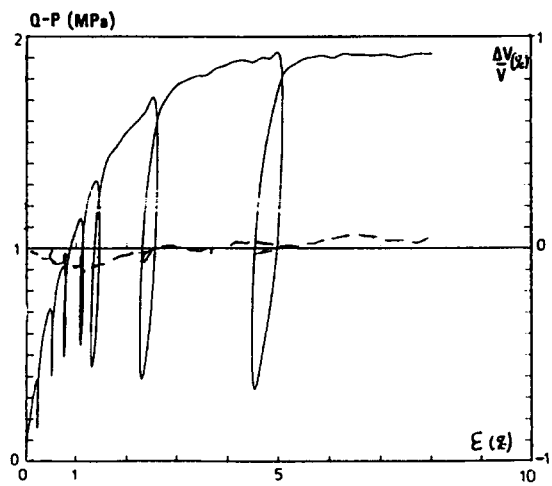

Fig. 4. Triaxial cyclic test on Boom clay.

remains after unloading (plasticity with strain hardening).

(b) Long term behaviour (isotropic state of total stress): The principal aspects are now studied of time-dependent behaviour of Boom clay by means of a special triaxial test performed at G.3S on a very accurate new device especially designed for the study of time-dependent phenomena [Fig. 5: triaxial drained/undrained test with pressure measurement in both porous plates (in undrained conditions) and measurements of the volume of displaced water (in drained conditions)].

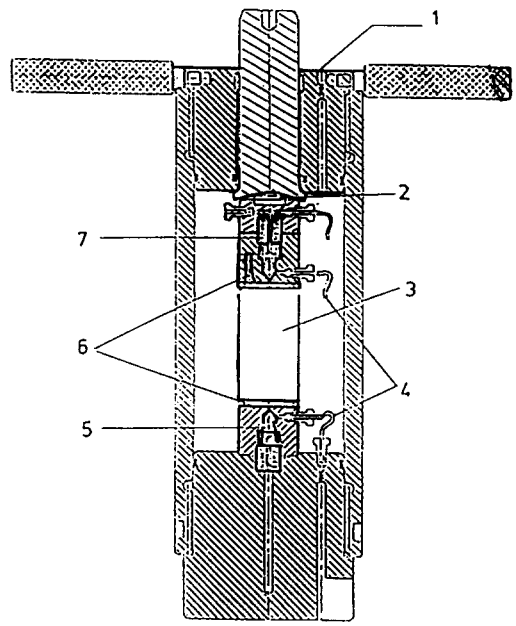

Fig. 5. Triaxial test for the measure of time dependent phenomena. *1*: Confining pressure, *2*: load sensor, *3*: sample, *4*: draining circuit, *5*: lower obturator, *6*: pressure sensor (p_l and p_u).

Fig. 6 summarises the results obtained in the first part of this test: the sample is submitted to an isotropic undrained loading–unloading path. We observe that the pore pressure equals the total stress loading. This result confirms a very well known property of saturated plastic clays, that the Skempton coefficient B_s is equal to 1.

In the second part of this test (Fig. 7), the isotropic condition for total stress is always maintained ($P=Q=5$ MPa), but the water pressure at the level of the lower porous plate is suddenly set to 2 MPa ($p_l=2$ MPa), although a no water flow condition is kept at the level of the upper plate.

The response of the sample consists of a progressive decrease of the water pressure p_u in the upper plate (diffusion process) and drainage of water through the lower plate, V_w. The time characteristic constant of this process is about 100 h (length of the sample: 72 mm).

Then, the loading is inverted (p_l is kept at 4.5 MPa); the symmetry of both curves $p_u(t)$ and $V_w(t)$ indicates that this total stress isotropic trans-

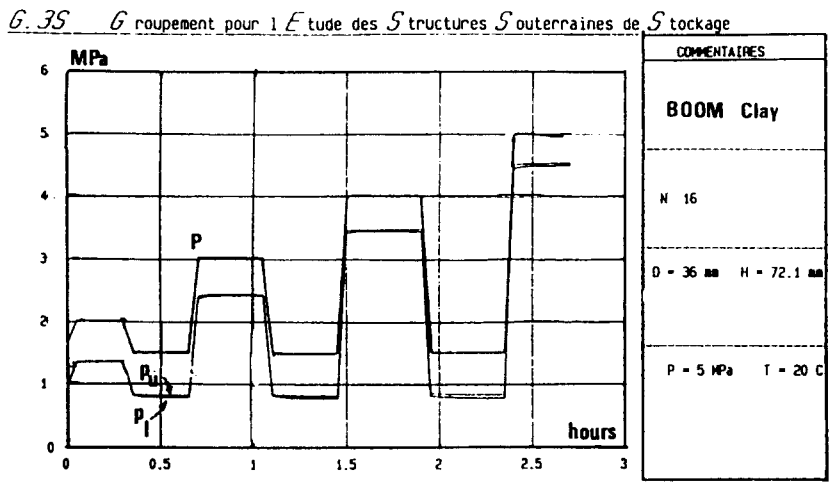

Fig. 6. Triaxial test on Boom clay, first part.

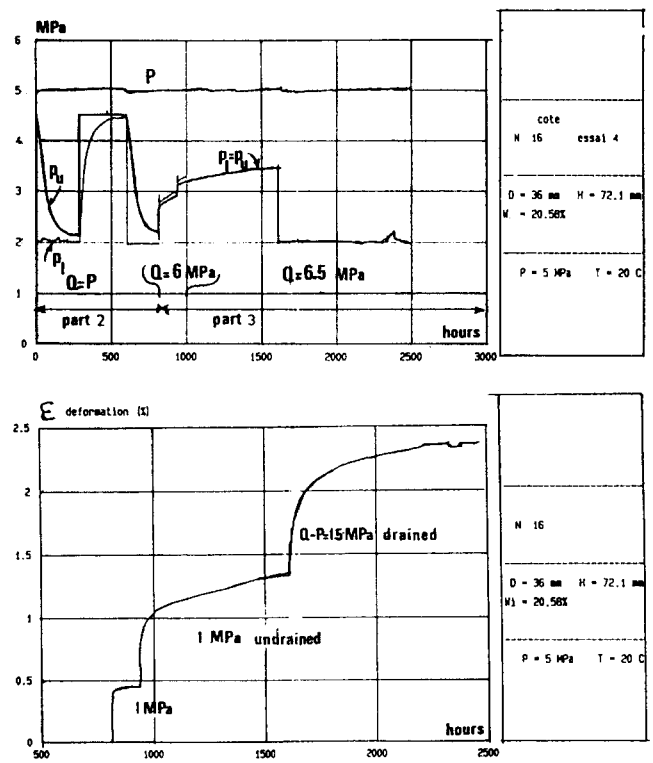

Fig. 7. Triaxial test on Boom clay, second and third part.

formation is reversible (see also the third and last step of this loading).

Under the 5 MPa isotropic total stress condition, by increasing water pressure within the sample from 2.0 to 4.5 MPa, the total volume of drained water is about 2500 mm^3, i.e., 3.4% of the total volume of the sample.

From this part of the test and from the triaxial

cyclic phase of the test, some characteristics of the reversible aspects of the behaviour of Boom clay can be deduced (if a linear elastic homogeneous and isotropic behaviour is assumed).

First, because $B_s \simeq 1$, we can suppose incompressibility of skeleton ($K_s = \infty$). So Biot's coefficients are:

$$b = 1 \qquad M = \frac{K_{fl}}{\phi_0} = 7333 \text{ MPa}$$

(with K_{fl} = compressibility of fluid = 3300 MPa, and ϕ_0 = porosity = 0.45).

During drainage under isotropic total stress, we have (see Coussy, 1989):

$$K_0/b = \delta p / \mathrm{Tr}\underline{\underline{\varepsilon}}$$

where δp = variation of pressure during the test (here $\delta p = 2.5$ MPa), and $\mathrm{Tr}\underline{\underline{\varepsilon}}$ = variation of the total volume (here $\mathrm{Tr}\underline{\underline{\varepsilon}} = 3.4\%$). So the drained bulk modulus of the porous medium K_0 is: $K_0 =$ 74 MPa.

The fourth and last coefficient necessary to describe the isothermal elastic behaviour of Boom clay is, for example, the undrained Young's modulus E, that can be deduced from the cyclic triaxial test: $E = 400$ MPa.

The relation between the undrained bulk modulus K and K_0, $K = K_0 + b^2 M$, allows to calculate K ($K = 7407$ MPa).

It is now easy to verify that Skempton's coefficient has a value near 1:

$$B_s = \frac{bM}{K} = 0.99$$

The other coefficients describing the elastic behaviour of Boom clay can be deduced from the four previous coefficients, b, M, K and E, by means of general relationships linking the parameters describing the porous medium. We find:

$\lambda_0 = 15$ MPa; $\lambda = 7318$ MPa; $G = 134$ MPa

(Lamé's constants)

$\nu = 0.491$; $\nu_0 = 0$

(Poisson's ratio; 0 for drained parameters).

Finally, the time characteristic of the drained part of the test can be related to permeability K_h by the following line of arguments.

The time characteristic of the diffusion equation can be written as: $\tau_h = a^2/D_h$, where D_h is the diffusivity and a is a dimension characteristic of the problem (here the length of the sample: $a =$ 7.2 cm). Generally, for elastic problems (see Giraud and Rousset, 1993):

$$D_h = \frac{K_h}{\gamma_w} \frac{M\,(3K_0 + 4G)}{3K + 4G}$$

So, $D_h = 2 \cdot 6\ 10^4\ K_h$ (K_h in m s^{-1}, D_h in m^2 s^{-1}) and finally: $K_h = 6 \cdot 10^{-13}$ m s^{-1}.

This value is in good agreement with other direct measurements of the permeability of Boom clay.

(c) Long term behaviour (deviatoric state of total stress): The third part of the specific test corresponds to a creep test ($P = 5$ MPa and $Q = 6$, then 6.5 MPa). At the beginning of this phase, the undrained sample is submitted to a deviatoric stress of 1 MPa (half of the maximum deviatoric stress representing the instantaneous strength of the material; moreover $P = 5$ MPa). One can observe that after a very short period of time, axial deformation does not evolve anymore. The second step ($Q - P = 1.5$ MPa), shows a time dependent behaviour always under undrained condition: axial deformation increases instantaneously from 0.5 to 0.8% and then from 0.8 to 1.3% in 600 h. All along this step, water pressure within the sample increases a little so that the mean effective stress goes slightly towards tension. This phenomenon is, however, not significant.

The main phenomenon here is that time dependent behaviour can be observed under undrained condition (the water pressure field is homogeneous within the sample). In other words, this delayed phenomenon cannot be explained by means of diffusion of water pressure.

For the last step of the test, the total stress field is the same as previously ($P = 5$ MPa, $Q =$ 6.5 MPa), but the drainage is open in the lower plate. The result is a sudden acceleration of deformation. After 100 or 200 h, the strain rate retrieves its previous value. This specific behaviour simply results first from consolidation of the material (water flow going out of the sample). The time

constant of this phenomenon is about 100 h, as found previously. Then, the time dependent behaviour cannot be explained by a Darcy's diffusion.

Other creep tests performed under high temperature show that the temperature has a very large influence on the creep: the threshold beyond which creep starts is smaller, creep rates are larger and failure strain is higher.

As a summary, the mechanical behaviour of Boom clay is characterised by the following:

— The instantaneous behaviour is plastic; ductility of the material is significant.

— The short term strength $(Q-P)_F$ is about 2 MPa.

— The behaviour is mainly irreversible even for very small strain (strain hardening phenomena).

— Time dependent behaviour of Boom clay is very significant and occurs even under undrained conditions (no pore water diffusion).

— For a permeability of about 10^{-12} m s^{-1} (if Darcy's law is assumed), for laboratory tests, the part of time dependent effects, due to a hydraulic diffusion process, lasts about 100–200 h. So, time dependent strains arising after this period (for a drained experiment) or those observed when performing undrained creep test, are related to the viscosity of the material.

— The long term threshold (in terms of deviatoric stress) beyond which time dependent strains develop is about $Q-P=1$ MPa (half the short term strength).

— Temperature has a great influence on the long term characteristics of Boom clay: the long term strength and the viscosity decrease when temperature increases.

2.2. The case of a brittle clay

Investigated is a deep marnous clay, cored at depths varying from 320 to 480 m in the Eastern part of the Parisian Basin. This material is less porous than Boom clay ($\phi \simeq 25\%$ compared to 45%) and its calcium carbonate content is about 20%.

Compared to Boom clay, this material is brittle (see for example the results of triaxial tests performed with $P=10$ MPa in Fig. 8). Failure happens for small values of axial strain of about $\varepsilon_F = 1.5\%$.

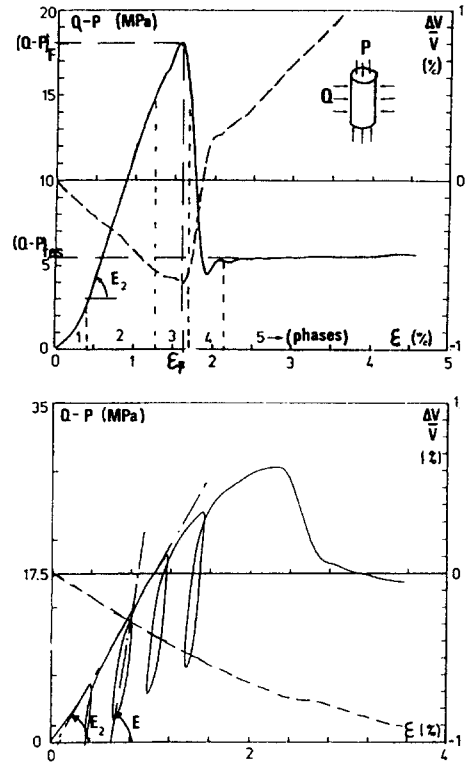

Fig. 8. Triaxial test on a brittle clay ($P=5$ MPa).

Nevertheless, creep of this material exists. On Fig. 9 is plotted an example of undrained creep tests results. For $Q-P<6$ MPa, strain rates always

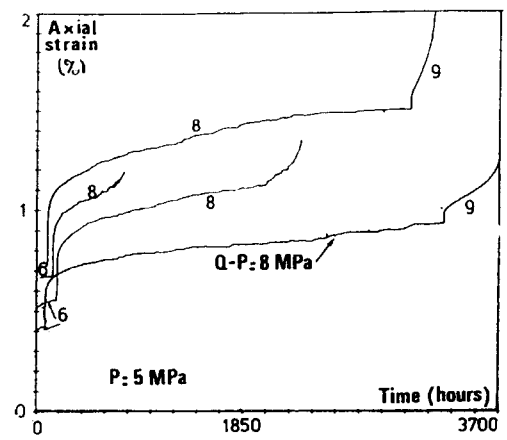

Fig. 9. Creep tests on a brittle clay.

vanish, so the viscoplastic threshold is greater than this value. For $Q-P=8$ MPa, we always observe a secondary creep phase. The strain rate during this phase is quite similar from one test to another; its value is $2\cdot10^{-6}\ \mathrm{h}^{-1}$. For $Q-P=9$ MPa, the secondary phase takes place at a larger rate and leads quickly to tertiary creep and failure. So, the long term failure limit of this material is determined as $Q-P=9$ MPa.

In all cases, long term failure occurs for a value of axial strain near 1.5%, similarly to short term failure. This is an important characteristic of the behaviour of the considered materials: independently of the rate of the loading process, macroscopic failure in triaxial tests arises at a constant axial deformation. The main features of the mechanical behaviour of this clay are: (a) short term behaviour is characterised by a significant brittleness, even at high confining pressures; (b) irreversible strains develop as soon as the material is loaded. The slope E of loading–unloading cycles (or Young's modulus), is two times greater than the slope E_2 of the $(Q-P)(\varepsilon)$ curve in its linear part; (c) despite a strong brittleness, these rocks exhibit a time-dependent behaviour under undrained conditions; (d) this long term behaviour is characterised by a non zero threshold and this limit is not sensitive to the mean stress level; (e) the long term failure axial strain is close to the short term, about 1.5%.

3. Constitutive models

As a possible constitutive model for plastic clay, to be able to take into account the main features of the thermo–hydro–mechanical behaviour previously illustrated (plasticity, diffusion, viscosity, etc.), a general thermo–poro–viscoplastic model is proposed in this section.

The quasistatic, infinitesimal deformations are considered of macroscopically homogeneous and isotropic fully saturated rocks with a connected pore structure. If solid and fluid phases are chemically inert and inertial forces negligible, the complete set of constitutive equations for linear reversible behaviour can be written:

$$\underline{\underline{\sigma}}=\underline{\underline{\sigma}}_\infty+\left(K-\frac{2}{3}G\right)\mathrm{tr}(\underline{\underline{\varepsilon}}-\underline{\underline{\varepsilon}}^{\mathrm{vp}})\underline{\underline{1}}+2G(\underline{\underline{\varepsilon}}-\underline{\underline{\varepsilon}}^{\mathrm{vp}})-bM\frac{m-m^{\mathrm{vp}}}{\rho^{\mathrm{fl}}_\infty}\underline{\underline{1}}-3\alpha K\theta\underline{\underline{1}}$$

$$P=P_\infty-bM\,\mathrm{tr}(\underline{\underline{\varepsilon}}-\underline{\underline{\varepsilon}}^{\mathrm{vp}})+M\frac{m-m^{\mathrm{vp}}}{\rho^{\mathrm{fl}}_\infty}+3\alpha_{\mathrm{m}}M\theta$$

$$S=S_\infty+3\alpha K\,\mathrm{tr}(\underline{\underline{\varepsilon}}-\underline{\underline{\varepsilon}}^{\mathrm{vp}})-3\alpha_{\mathrm{m}}M\frac{m-m^{\mathrm{vp}}}{\rho^{\mathrm{fl}}_\infty}+\frac{C\varepsilon}{T_\infty}\theta\qquad(\theta=T-T_\infty)$$

The independent state variables in elasticity are $\underline{\underline{\varepsilon}}^{\mathrm{e}}=\underline{\underline{\varepsilon}}-\underline{\underline{\varepsilon}}^{\mathrm{vp}}$, $m^{\mathrm{e}}=m-m^{\mathrm{vp}}$ and T, respectively the elastic linearized strain tensor, the elastic fluid mass supply related to the initial volume (Coussy, 1989) and the temperature (see also Biot, 1941, 1955; Rice and Cleary, 1976; Kümpel, 1991 for significance of poroelastic parameters). The associated variables are the Cauchy stress tensor $\underline{\underline{\sigma}}$, the pore pressure field P and the entropy S. For the irreversible part of the behaviour studied here, two new variables must be added: the current vicsoplastic strain tensor $\underline{\underline{\varepsilon}}^{\mathrm{vp}}$ and the irreversible fluid mass supply m^{vp}. The dissipations of heat and hydraulic mass obey the linear Fourier's and Darcy's laws.

The simplest thermoporoelastic model contains nine independent parameters: four parameters in isothermal condition (for example, the undrained bulk modulus K, the shear modulus G, the Biot coefficient b and the Biot bulk modulus M); three parameters in non isothermal conditions (the linear undrained dilatation coefficient α, the differential dilatation coefficient α_{m} and C_ε, specific heat); and two parameters for the Fourier's and Darcy's laws (the thermal conductivity λ_{T} and the hydraulic permeability K_{h}). The viscoplastic porosity ϕ^{vp} is now defined by $\phi^{\mathrm{vp}}=m^{\mathrm{vp}}/\rho^{\mathrm{fl}}_\infty$. We assume in this paper the hypothesis of viscoplastic effective stresses (Coussy, 1989) which means that the irreversible variation of porosity ϕ^{vp} is proportional to the viscoplastic volumetric strain $\mathrm{Tr}(\underline{\underline{\varepsilon}}^{\mathrm{vp}})$:

$\phi^{vp} = \beta \, \mathrm{Tr}(\underline{\underline{\varepsilon}}^{vp})$

According to creep test results, to describe viscoplastic behaviour, a Bingham's model with a viscoplastic threshold that does not depend on the main stress (Tresca's limit) is chosen:

$$\underline{\underline{\dot{\varepsilon}}}^{vp} = \frac{1}{\eta} \langle |\sigma_1 - \sigma_3| - 2C \rangle^n \quad \partial g(\underline{\underline{\sigma}})/\partial \underline{\underline{\sigma}}$$

($\sigma_1 > \sigma_2 > \sigma_3$: principal stresses)

Three new parameters appear: η skeleton viscosity, C cohesion, and n non linearity exponent (so, this constitutive model for Boom clay contains twelve parameters).

The hypothesis of a Tresca criterion and effective stresses imply that there is no irreversible variation of porosity. This property does not fit very well with experimental results and a further improvement of the constitutive model for Boom clay may include a better estimation of irreversible strains under isotropic stress conditions.

Effects of temperature on the long term properties of clay can be taken into account by choosing specific variations of cohesion and viscosity $\dot{C}(T)$ and $\eta(T)$ ($\dot{C} < 0$ and $\dot{\eta} < 0$). An identification of the twelve parameters of this model, by means of the experimental results presented above leads to the values given in the first column of Table 1.

The second column of Table 1 gives another set of parameters, rather close to the previous one, which will be used further for the calculations of the effects of a heating source in Boom clay (Giraud, 1993).

The elastic parameters K_0, G and M are strongly different between the second column and the first column. Parameters of the first column are identified by means of the experimental results presented above, while the parameters of the second column are similar to the values taken into account by Picard et al. (1991) for studying in situ tests on Boom clay.

Finally, in the third column, the parameters of an athermal poro-plastic model for Boom clay, which has been considered for the Interclay II European exercise are given. This last model is used further for the parametric study of the lined tunnel in porous medium (CEC, 1992).

For a brittle clay, in addition to viscoplastic behaviour, for many applications, the short term failure is taken into account. A natural way to treat this difficult coupling is to add a brittle element to the viscoplastic one.

The main interests of this viscoplastic-with-failure constitutive model, illustrated on Fig. 10, are given in Nguyen Minh and Rousset (1987).

4. Applications

Numerical calculations exposed in this paper have been performed using the numerical computer code THYME (Giraud, 1993). THYME is an one

Table 1
Parameters of the poro-viscoplastic model for Boom clay

	Boom clay		Interclay II
Drained bulk modulus K_0 (MPa)	74	500	250
Shear modulus G (MPa)	134	511	80
Biot coefficient b	1	0·82	1
Biot bulk modulus M (MPa)	7333	2830	5500
Permeability K_h (m s^{-1})	$6{\cdot}10^{-13}$	$4{\cdot}10^{-12}$	$4{\cdot}10^{-12}$
Specific heat C_ε^0 (J m^{-3} K^{-1})		$2{\cdot}82{\cdot}10^6$	
Drained coefficient of thermal dilation α_0 (K^{-1})		10^{-5}	
Undrained coefficient of thermal dilation α (K^{-1})		$4{\cdot}48{\cdot}10^{-5}$	
Thermal conductivity λ_T (W m^{-1} K^{-1})		1·7	
Cohesion C (MPa)	0·5	0·5–0·2	1
Viscosity η (MPa^n days)		100	
Non linearity exponent n		4	

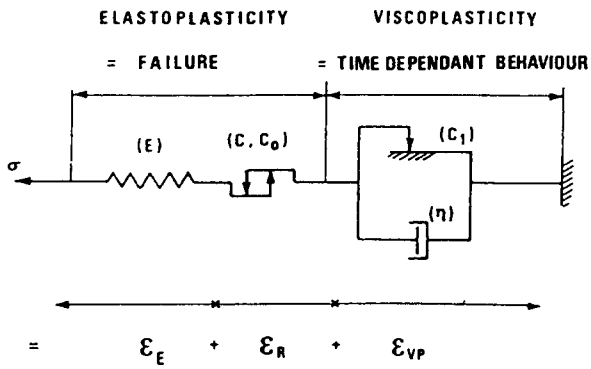

Fig. 10. Viscoplastic-with-failure model.

dimensional code for porous media, using the finite element method.

Hermite polynomial basis functions are used, so the nodal unknowns are the displacements, pore pressure, temperature and their first spatial derivatives.

Two applications of the constitutive models exposed in the previous chapter are given in this paper. We first study the time dependent behaviour of a tunnel excavated in deep clays (assuming isothermal conditions) and then, we study the time dependent behaviour of a pile of heat emitting canisters buried in the Boom clay.

4.1. Time dependent behaviour of a tunnel excavated in a deep clay

We are interested in the axisymmetrical problem of a deep circular tunnel (radius r_i) in an isotropic homogeneous medium, previously in a state of uniform stress $\sigma_{ij}^{\infty}=\sigma_{\infty}\delta_{ij}$ and constant pore pressure $p=p_{\infty}$. Disregarding the effects due to progressive excavation, plane strain assumption allows an one-dimensional study.

The problem is first simplified neglecting the viscosity of the solid skeleton. The constitutive model considered first is simple: poro-elastoplastic model (first column of Table 1), which allows to study time dependent behaviour only due to hydraulic diffusion. After this first study, the viscosity of the solid skeleton is considered and the relative effects of hydraulic diffusion and viscosity on the delayed behaviour of the structure are examined.

Stage one: excavation phase. The circular tunnel is excavated and the effect of the retreating excavation front is simulated by an instantaneous variation of the inner radial stress at the tunnel wall from σ_{∞} to a final prescribed value σ_i (see Fig. 11), corresponding to the pressure acting on the lining at the end of the construction of the tunnel. As we will see later, the assumption of instantaneous loading for this phase is valid, because the time needed for the excavation of a tunnel is smaller than the characteristic time constant τ_h of the hydraulic diffusion (see later).

Stage two: time-dependent behaviour. After the previous mechanical loading, the structure is now submitted to the effect of hydraulic diffusion within the rock mass. In particular, the ultimate pore pressure distribution depends on the hydraulic behaviour of the lining. We have studied two different evolutions corresponding to two different hydraulic boundary conditions which may represent two opposite cases encountered in practice: fully drained hydraulic boundary condition $(p(r_i,t)=0)$ corresponds to a permeable lining and undrained hydraulic boundary condition $(\partial p(r_i,t)/\partial r=0)$ corresponds to an impervious lining.

Apart from the hydraulic boundary condition, the time-dependent behaviour is also closely linked to the mechanical behaviour of the lining. For the gallery lined with sliding ribs previously described, the pressure acting on the tunnel wall may be considered as constant, while convergence develops. On the other hand, a rigid lining does not allow any convergence, but it supports an increase of mechanical pressure. The sliding ribs lining is modelled further by the following loading path case refered as the "creep" case for which σ_i remains constant during the entire process (see

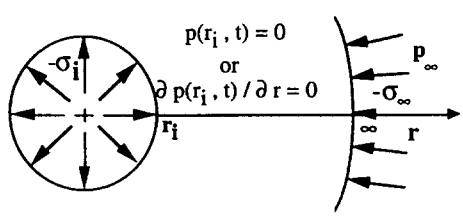

Fig. 11. Loading and boundary conditions.

Giraud and Rousset, 1993 for the study of the rigid lining).

Calculation parameters. Calculations given for this application have been done using parameters values (given in Table 1) proposed for the benchmark Interclay II. One plastic model is considered in this paper: a Tresca model ($\phi = 0°$, $C = 1$ MPa) (see Giraud and Rousset, 1993; and Giraud, 1993 for parametrical study taking into account Mohr–Coulomb models). Initial conditions correspond to a 250 m deep tunnel: $\sigma_\infty = -5$ MPa and $p_\infty = 2.5$ MPa. The tunnel radius r_i is taken equal to $r_i = 2.5$ m and the inner radial stress $\sigma_i = -2.5$ MPa.

Results. The results are presented hereafter in a dimensionless form. First we define the characteristic hydraulic diffusion time τ_h:

$$\tau_h = \frac{r_i^2}{D_h} \qquad (\tau_h = 2.13 \text{ years})$$

So, this first problem is characterised by only one characteristic time: the characteristic hydraulic diffusion time τ_h.

Normalized radius r' and normalized time t' are respectively: $r' = r/r_i$ and $t' = t/\tau_h$. Radial convergence $U_i = -u(r_i,t)/r_i$, normalized pore pressure $p' = p/p_\infty$, normalized inner radial stress at the tunnel boundary $\sigma'_i = \sigma_i/\sigma_\infty$, normalised boundaries of plastic zone $y' = y/r_i$ and $x' = x/r_i$ are the other dimensionless parameters of this problem.

Excavation phase. The excavation generates a plastic zone close to the tunnel wall, in which pore pressure drops, while the outer zone remains elastic. As was noted previously (see Fig. 12), this phenomenon corresponds to in situ observations: the piezometer located near the cavity showed an instantaneous drop of pore pressure. No pore pressure variation develops in the elastic zone, which is not surprising because in linear elasticity, excavation in an infinite medium is locally an isocoric process (see Fig. 12, $\sigma'_i = 0.5$).

Time dependent behaviour. Just after the excavation, the pore pressure distribution is not uniform within the rock mass. Thus, whatever the mechanical and hydraulic boundary conditions, fluid flow occurs within the rock mass, causing time dependent changes for the structure.

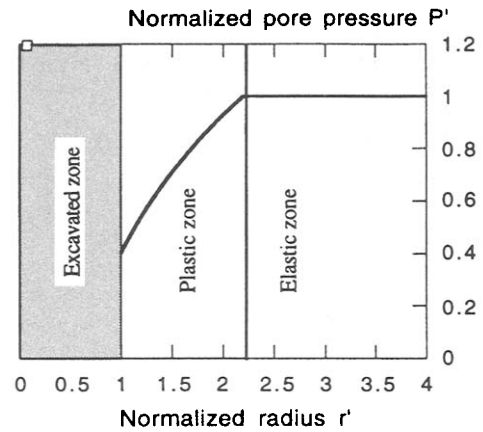

Fig. 12. Normalized pore pressure p' after the excavation phase.

The ultimate pore pressure distribution differs whether the lining is impervious or not. For undrained conditions, the ultimate distribution is constant, whereas for drained conditions, pore pressure tends to a log type profile. In the first case the pore pressure in the plastic area increases and in the second case, decreases (see Fig. 13).

Due to the absence of evolution in the mechanical equilibrium expressed in terms of total stress, it may be noticed that total stress variations within the rock mass are limited. Because of the change of pore water pressure field previously described, the effective stress change tends towards tension in case of an impervious lining, and towards compression in case of a permeable lining. The numerical results confirm this qualitative analysis. Indeed, only very small convergence develops in the drained case (see Fig. 14). On the contrary, the undrained case show high time dependent convergence. Calculations show that time dependent convergence represents approximately 25% of the ultimate convergence.

More can be learned by studying the curves showing the evolution of the plastic zone boundary (see Fig. 15).

In the drained case, the outer radius of this zone decreases and after a certain time, all the rock mass behaves elastic. Consequently, plastic flow is

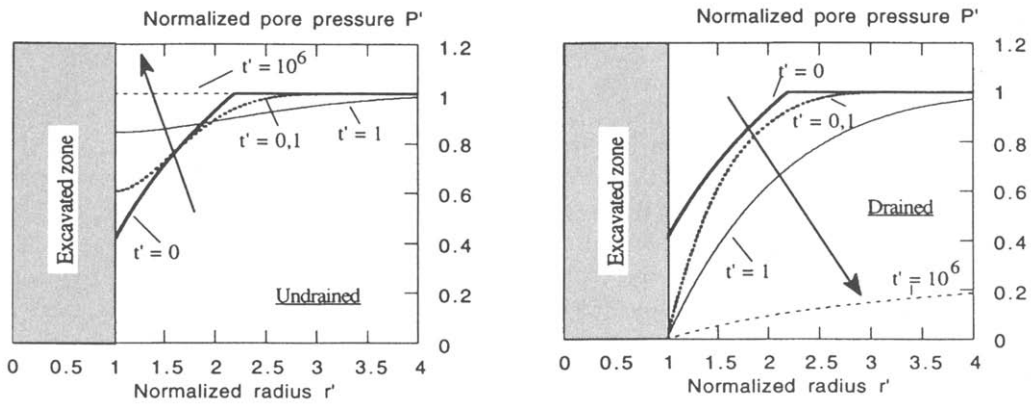

Fig. 13. Profiles of normalized pore pressure p'.

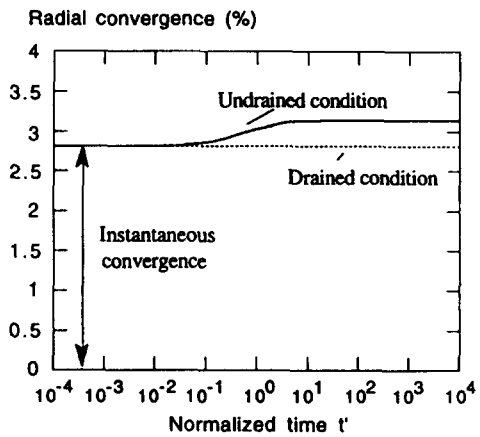

Fig. 14. Radial convergence evolution.

low for the drained case, and the total amount of time dependent convergence remains limited. The evolution is more complex for the undrained case: first, the boundary of the plastic zone diminishes, but after small time values, it extends notably. A stabilisation can be noticed and the ultimate extension of the plastic zone shows that the mechanical behaviour of the rock mass near the tunnel is irreversibly modified by the hydraulic diffusion process.

The evolution near the tunnel wall is, therefore, rather complicated: it consists of a succession of plastic loading, elastic unloading and sometimes plastic reloading, due to the pore pressure diffusion.

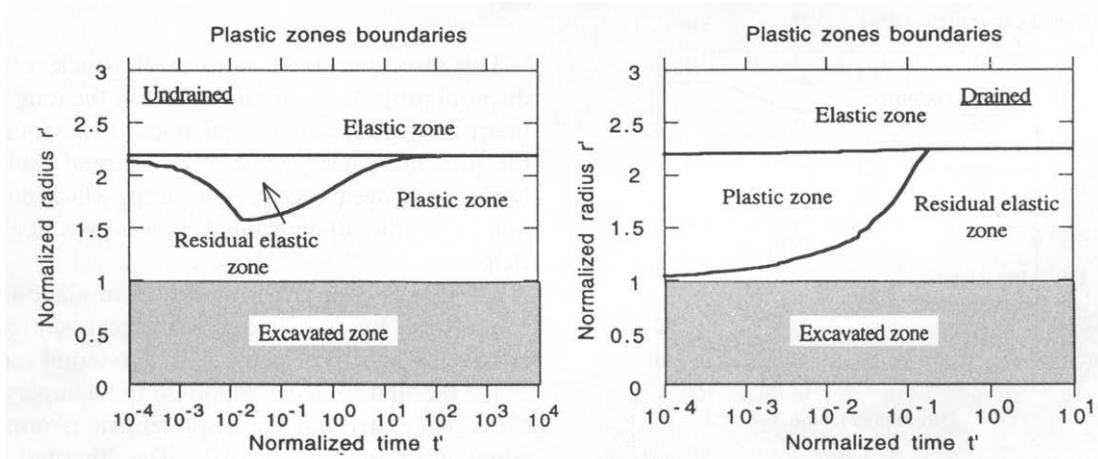

Fig. 15. Plastic zones evolution.

Viscosity and hydraulic diffusion: poro-elasto-viscoplasticity. As an extension of the previous analysis and in order to take into account the viscosity of the solid skeleton we have studied the case of the imperviously lined tunnel in a poro-elasto-viscoplastic model (for the same Tresca criterion). This constitutive model is that of Bingham (a linear dash pot is in parallel with the sliding element). The only additional parameter of this model is viscosity η; when $\eta \to 0$, the previous poro-elasto-plastic model is again found.

The problem can be defined now with two characteristic times: the characteristic hydraulic diffusion time τ_h and the characteristic viscosity time τ_η:

$$\tau_\eta = \frac{\eta\,(1-\nu_0)}{E_0}$$

The "creep" test is illustrated on Fig. 16. Plotted is the convergence U_i versus normalized time for the poro-elastic-plastic model (P) (the same as in Fig. 14) and the poro-elastic-viscoplastic model (VP). The differences between both evolutions is very marked at the beginning of the process. The response of the VP model at the first instantaneous stage is purely elastic because viscosity prevents any plastic strain. Then the evolution is explained of two different parts: first, convergence evolves due to viscous process, then time dependent effects are due to hydraulic diffusion. So, in the case of this particular VP model, the magnitude of time dependent closure is mainly due to the viscous cause (range of 60%; 40% being due to the hydraulic diffusion process).

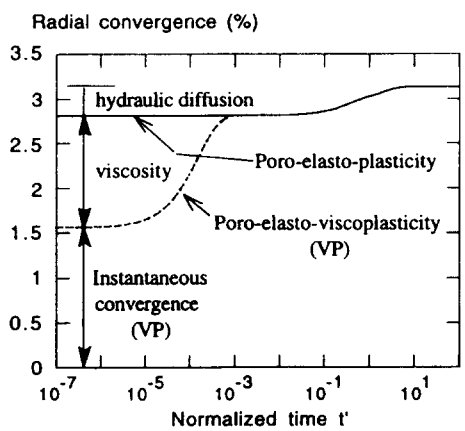

Fig. 16. Radial convergence evolution: comparison between plastic and viscoplastic behaviours.

Conclusion. The two main factors responsible for time dependent behaviour of a circular tunnel excavated in poroplastic media such as clay are the nature of the hydraulic boundary condition at the tunnel wall (nature of the lining) and the plastic properties of the clay mass.

For Tresca models, the choice of a permeable lining (which corresponds to a drained hydraulic boundary condition) leads to negligible time dependent convergence.

An impervious lining can lead to important delayed convergence and plastic evolutions depending on the mechanical loading applied and on the viscoplastic properties of the clay mass. For the Tresca model, exhaustive parametric studies presented in Giraud (1993) show that the time-dependent convergence is about 40% of the instantaneous convergence for the Boom clay.

The main conclusions (important delayed convergence for impervious lining, and small time dependent effects for permeable lining) can be extended (Giraud, 1993) for plastic criteria such as Mohr–Coulomb and modified Cam Clay.

4.2. *Behaviour of a pile of canisters buried in a deep clay*

This second problem concerns the nuclear waste disposal project. We are interested in the long term thermal-hydraulic and mechanical behaviours of the rock mass near a pile of exothermal canisters buried in a deep clay (230 m deep, which corresponds to the underground laboratory at Mol, Belgium).

The pile of canisters is modelled, in plane strain conditions, by a cylindrical thermal source of infinite length and of radius r_i. The external surface of the thermal source is supposed to be impervious ($\partial P(r_i,t)/\partial r = 0$) and the displacement is imposed equal to zero ($u(r_i,t)=0$). The thermal flux imposed at $r=r_i$ decreases exponentially as a char-

acteristic of the nuclear wastes:

$$\frac{\partial T(r_i,t)}{\partial r} = -Q_{\Pi}\frac{e^{-\omega t}}{2\pi\lambda_T r_i}$$

(λ_T represents the thermal conductivity and ω the decay constant of exponential decrease law).

The only loading considered is thermal. In particular, we do not consider the excavation phase.

The constitutive model is the thermal-poro-viscoplastic model which has been exposed in section 3 (values of the parameters are given in the second column of Table 1). The influence of the temperature on the delayed behaviour of the structure is studied by means of a parametrical study on the cohesion. Different values of cohesion between $C=0.5$ MPa and $C=0$ MPa are considered (which corresponds to the limit case of a material without cohesion) as well as negative hardening of cohesion versus temperature.

Compared to the previous application, the problem of the behaviour of a pile of canisters is defined by two more characteristic times: the thermal diffusion characteristic time τ_T and the characteristic time of the thermal loading τ_ω ($\tau_\omega = 1/\omega$ and $\tau_T = r_i^2/D_T$ where D_T denotes the thermal diffusivity $D_T = \lambda_T/C_\varepsilon^0$).

Because of the non linearity of the viscosity of this model, the viscoplastic characteristic time τ_η has to be defined with a new viscosity η' which is a linear viscosity, equivalent to the viscosity η in the case of a linear viscoplasticity ($\eta' \sim 10^4$–$2\cdot10^4$ MPa days).

So this problem is now defined by four characteristic times: hydraulical τ_h, viscoplastic τ_η, thermal τ_T and τ_ω (see Table 2). The multiplicity of the characteristic times makes the analysis of the problem difficult. Calculations and analyses show that the variation of one characteristic time strongly affects the delayed behaviour of the structure (for example, a variation of permeability from $4\cdot10^{-12}$ m s^{-1} to $4\cdot10^{-13}$ m s^{-1} implies a variation of the characteristic hydraulic diffusion time τ_h from 4.8 days to 48 days).

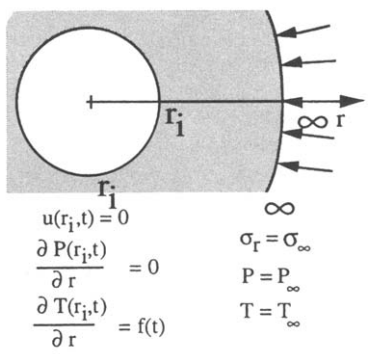

Fig. 17. Boundary conditions and geometry.

The three characteristic times τ_η, τ_h and τ_T are of the same order of magnitude and negligible compared to τ_ω. The extrinsic nature of the characteristic hydraulic diffusion time τ_h appears clearly if we compare the value of τ_h defined for the previous problem ($\tau_h = 800$ days) to the new value of $\tau_h = 4.8$ days. The value of the permeability is the same for both models, the differences encountered in the values of τ_h are mainly due to the dimensions of the structures studied: first a tunnel of radius $r_i = 2.5$ m and second a borehole of radius $r_i = 0.215$ m.

The evolutions of temperature, pore pressure and mean stress σ_m at the point located at the radius $r' = 2r_i = 0.43$ m are exposed in Figs. 18, 19 and 20.

Due to the particular thermal loading of the nuclear wastes, temperature first increases within the rockmass near the pile and then, there is a cooling of the rockmass (linked to thermal decreasing). The maximum of temperature elevation is reached after 2500 days and its value is of 100°C at the point $r' = 2$ (Fig. 18).

We compare, at the same point $r = 2r_i$, the evolution of pore pressure (Fig. 19) corresponding to the viscoplastic media (for cohesion $C=$ 0.5 MPa, and $C=0$) and the elastic medium. Maxima of pore pressure elevation are important, of the same order of magnitude than the initial

Table 2
The four characteristic time constraints

Characteristics time constraint	Value (days)
Thermal diffusion τ_T	3·6
Hydraulic diffusion τ_h	4·8
Viscoplastic τ_η	7·7
Thermal loading τ_w	$1{\cdot}5{\cdot}10^4$

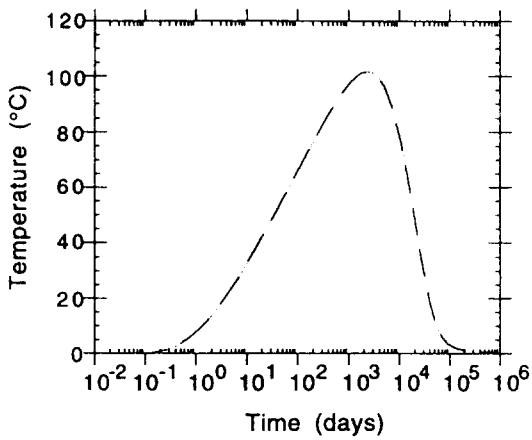

Fig. 18. Temperature evolution.

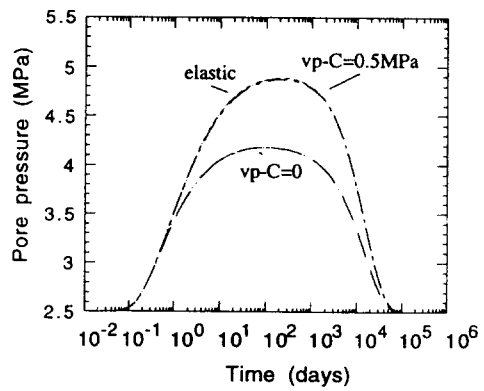

Fig. 19. Pore pressure evolution.

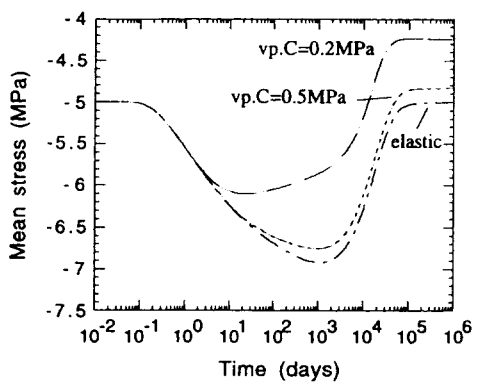

Fig. 20. Total mean stress evolution.

value (2.4 MPa for the elastic and viscoplastic medium $C=0.5$ MPa). In the particular case of the viscoplastic medium without cohesion, maximum of pore pressure elevation are nearly 30% lower than in the elastic case. So, for the constitutive model we have considered, the effect of viscoplasticity on the pore pressure dissipation is quite small.

The evolution of total mean stress σ_m at $r'=2$ (Fig. 20) shows that residual stresses appear in the viscoplastic media ($C=0.2$ MPa, and $C=0.5$ MPa) after the cooling of the structure. This phenomenon is significant (a residual variation of traction of 0.9 MPa, 20% of the initial stress develops in the viscoplastic medium $C=0.2$ MPa) and traduces an irreversible modification of the behaviour of the rock mass near the pile of canisters.

5. Conclusions

Coupling effects between thermal, hydraulic and mechanical behaviours are very strong in low permeable deep clays (saturated compressible clays with high porosity such as Boom clay). Calculations show that displacements and stresses are very sensitive to the constitutive model. The appearance of residual stresses and viscoplastic zones in the rock mass near the pile of canisters illustrate the global irreversible behaviour of the structure.

References

Bernaud, D. and Rousset, G., 1993. L'essai de soutènement à convergence contrôlée: Résultats et Modélisation. Int. Symp. Hard Soils — Soft Rocks, Athens.

Biot, M.A., 1941. General theory of three-dimensional consolidation. J. Appl. Phys., 12: 155–164.

Biot, M.A., 1955. Theory of elasticity and consolidation for a porous anisotropic solid. J. Appl. Phys., 26: 182–185.

C.E.C., 1992. Interclay II Project — Preliminary Results For Benchmarks 1. WS Atkins Science & Technology, U.K.

Coussy, O., 1989. A general theory of thermoporoelastoplasticity for saturated porous materials. Transp. Porous Media, 4: 281–293.

Coussy, O., 1991. Mécanique des Milieux Poreux. Technip Paris.

Giraud, A., 1993. Couplages thermo-hydro-mécaniques dans

les milieux poreux peu perméables: Application aux argiles profondes. Ph.D. thesis, E.N.P.C., Paris.

Giraud, A. and Rousset, G., 1993. Comportement thermo-hydro-mécanique d'un puits de stockage de déchets radioactifs dans une argile profonde. In: R.E. Sousa and Grossmann (Editors), Safety and Environmental Issues in Rock Engineering. Balkema, Rotterdam, Vol. 1: 293–301.

Giraud, A., Picard, J.M. and Rousset, G., 1993. Time dependent behaviour of tunnels excavated in porous rock mass. Int. J. Rock. Mech. Min. Sci.; Geomech. Abstr., 30(7): 1953–1959.

Kümpel, H.J., 1991. Poroelasticity: parameters reviewed. Geophys. J. Int., 105: 783–799.

Neerdael, B., De Bruyn, D., Mair, R.J. and Taylor, R.N., 1991. Geotechnical behaviour of Boom Clay. Comm. Eur. Commun., Nuclear Science and Technology, Pilot Tests on Radioactive Waste Disposal in Underground Facilities. EUR 13985 EN, pp. 223–238.

Nguyen Minh, D. and Rousset, G., 1987. Influence of instantaneous failure on time-dependent behavior of underground galleries. 28th U.S. Symp. Rock Mechanics. Univ. of Arizona, Tucson, Ariz.

Picard, J.M., Bazargan, B., Rousset, G. and Vignal, B., 1991. The CACTUS in-situ test: behavior of Boom clay under thermal loading. Comm. Eur. Commun., Nuclear Science and Technology, Pilot Tests on Radioactive Waste Disposal in Underground Facilities. EUR 13985 EN., pp. 255–264.

Rice, J.R. and Cleary, M.P., 1976. Some basic stress diffusion solutions for fluid saturated elastic porous media with compressible constituents. Rev. Geophys. Space Phys., 14: 227–241.

Rousset, G., 1988. Comportement mécanique des argiles profondes — Application au stockage de déchets radioactifs. Ph.D. thesis, ENPC, Paris.